A stable α-lactam reagent for bioconjugation and proteomic profiling

Alejandro Mahía[1], Anders E. Kiib[1], Marija Nisavic[1,2], Johan Palmfeldt[2], Thomas B. Poulsen[1,*]

[1] Department of Chemistry, Aarhus University, Langelandsgade 140, DK-8000, Aarhus C, Denmark.

[2] Department of Clinical Medicine—Research Unit for Molecular Medicine, Aarhus University hospital,
Palle Juul-Jensens Boulevard 82, DK-8200 Aarhus N, Denmark

[*] e-mail: thpou@chem.au.dk

ABSTRACT

Electrophilic groups are one of the key pillars of contemporary chemical biology and medicinal chemistry, constituting the anchor point for the design of targeted covalent inhibitors, the identification of novel therapeutic targets, and the development of a wide diversity of bioconjugation and proteomic profiling techniques. Naturally, there is great interest in the discovery of new types of biologically relevant electrophiles with potent action and broad applicability. For instance, the group of 3-membered *N*-heterocyclic compounds - such as aziridines, azirines, and oxaziridines – combine unique electronic properties and structural strain to trigger their respective potential and applicability as covalent tools. The α-lactams are also members of this group of compounds, but, until this point, their utility within the field has been unexplored. Here, we demonstrate an α-lactam reagent that can be efficiently employed in the framework of bioconjugation and proteomic profiling. We have designed and synthesised a stable α-lactam, **AM2**, that is compatible with aqueous buffers, and have extensively characterised its properties and reactivity. In simple settings, **AM2** was e.g. found to be reactive towards both thiols and amines, with the former reacting significantly faster. We further demonstrated that **AM2** undergoes conjugation to free cysteine residues in peptides suggesting applications for bioconjugation. Interestingly, liver carboxylesterase 1 (CES1), a serine hydrolase with key roles in both endo- and xenobiotic metabolism, was found as a highly selective covalent target for **AM2** in HepG2 liver cancer cells. All in all, our study constitutes the starting point for the further development of α-lactam-based electrophilic probes and exploration of their use in covalent chemical biology.

INTRODUCTION

Electrophilic functional groups are a corner stone of covalent chemical biology and contemporary medicinal chemistry. For instance, targeted-covalent inhibitors (TCIs), which rely on the fusion of weakly-reactive electrophiles with optimised protein-binding scaffolds, can have favourable pharmacodynamic properties, such as prolonged residence times.[1–3] In comparison, structurally simpler compounds - fragments - that still incorporate reactive groups, are increasingly employed in chemical genetic screens for discovery of novel targets or ligandable sites.[4–8] The combination of scaffold structure and intrinsic reactivity of the electrophilic group, defines the compounds' unique interactions across the proteome. Finally, reagents that comprise mainly a reactive group alone, along with an affinity/visualisation tag, enable broad, residue-specific, proteomic profiling experiments to be conducted. Since the seminal reports on fluorophosphonate activity-based probes for serine hydrolase profiling,[9,10] proteomic profiling technology has expanded in scope and sophistication to address an ever larger part of the (reactive) proteome and has furthermore become a key method for target identification through competitive chemical proteomics.[4,11–13] As a separate area of application, many bioconjugation methods also rely on electrophilic agents with the aim of achieving selective biomolecular labelling with residue- or sequence-specific resolution. The introduction of new electrophilic motifs can therefore have broad impact and this is an area that we,[14,15] as well as many others,[16–23] have been recently pursuing.

Within the portfolio of potentially biologically relevant reactive groups, 3-membered *N*-heterocycles are privileged due to their unique electronic properties and significant structural strain (Figure 1a). For instance, aziridine-derivatives have been used as covalent inhibitors of glycosidases since the last 35 years,[24] and this scaffold was also recently demonstrated to selectively react with carboxylate residues in proteins[25] (Figure 1a, top left). Redox-activated chemical tagging employing oxaziridines as reactive probes has emerged in the last years as a novel and robust strategy for the chemoselective bioconjugation of methionine residues with potential applications in the synthesis of antibody-drug conjugates, peptide stapling or proteomic profiling of functional methionines in cells[26,27] (Figure 1a, bottom left). Very recently, azirine-based reagents were demonstrated to also enable chemoselective functionalisation of carboxyl residues in proteins (Figure 1a, bottom right).[28] In contrast, the related diazirine-ring system does not possess any relevant electrophilic reactivity but is instead widely employed in photoaffinity labelling of targets *via* light-induced generation of a reactive carbene (Figure 1a, top right).[29] Interestingly, it has recently been reported that alkyl diazirines react preferentially with acidic amino acids through a reactive diazo intermediate, which causes increased selectivity for membrane proteins and proteins with large negative electrostatic surfaces.[30] Yet, within the above-mentioned framework of (chemical) biological applications of 3-membered *N*-heterocycles a fundamental member is missing: the α-lactams (Figure 1b). The absence of any known utility, or biological role, of α-lactams can probably be attributed to the widely reported instability of this ring system,[31] which is interesting given the close resemblance to the ubiquitous β-lactam structure present e.g. in the major antibiotics of the penicillin and cephalosporin classes, working through covalent inhibition of transpeptidase enzymes.[32]

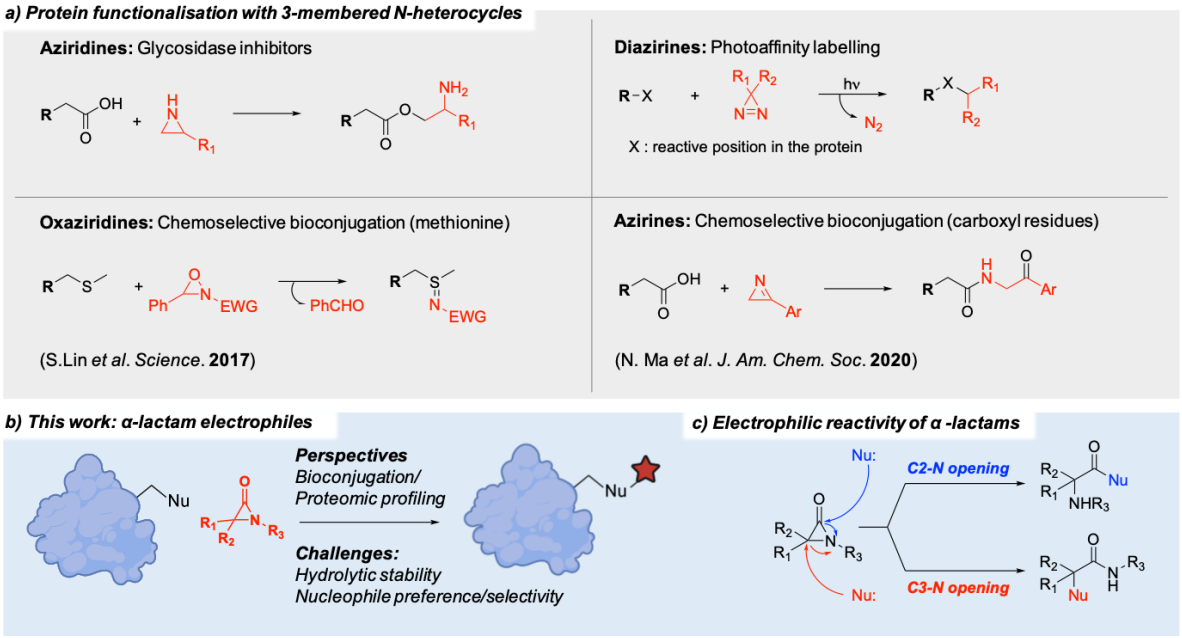

Figure 1. a) Classic and more recent examples of 3-membered N-heterocycles employed as reactive probes for different applications in chemical biology. b) Potential applicability of α-lactams as electrophilic reagents in chemical biology. c) Reaction modes of α-lactams with nucleophiles.

α-Lactams have been postulated as chemical intermediates in numerous reaction mechanisms[31] and the first isolation of an α-lactam (*N-tert*-butyl-3-phenylaziridinone) from reaction media was accomplished in 1962.[33] Since, other examples have been synthesised and isolated from which a general stability trend can be inferred: α-lactams that feature a tertiary alkyl or cycloalkyl group attached to the amide nitrogen atom along with the presence of a tertiary alkyl or a phenyl group at C3 display enhanced stability.[34] In this regard, the isolatable α-lactam 1,3-di-*tert*-butylaziridinone has been reported to have surprisingly high thermal stability and greater resistance to nucleophilic attack, requiring several days in refluxing methanol to complete solvolysis.[34,35] Fundamentally, α-lactams undergo two different types of ring-opening reactions with nucleophiles: C2-N opening that generates 2-amino acyl derivatives and C3-N opening that generates 2-substituted amides (Figure 1c). The factors that govern the regioselectivity of the nucleophilic attack are not completely understood and both the structure of the α-lactam and the nature of the nucleophile (in terms of strength and type) affect the final outcome of the reaction.[36–39] Nevertheless, a general, simple and illustrative ruleset can be established as follows: strong nucleophiles like alkoxides and non-sterically hindered amines favour C2-N opening of α-lactams, while weaker nucleophiles like water, alcohols, halides and sterically hindered amines tend to generate C3-N opening products.

We questioned whether an α-lactam could be prepared with sufficient stability to resist fast hydrolysis in aqueous media while maintaining reactivity towards nucleophilic amino acids (Figure 1b). Given the unique structure and reactivity associated with the α-lactam ring as outlined above, such a compound would constitute a novel electrophile for covalent chemical biology. Here, we report the preparation of an α-lactam derivative that is compatible with

aqueous buffers along with an in-depth study of its reactivity. We also demonstrate its use for peptide functionalisation and as an electrophilic probe in cells and cell lysate.

RESULTS AND DISCUSSION

Synthesis of α-lactam derivatives

Taking into account the previously described indicators for stability of α-lactams, we initially selected the compound **AM1** with a *t*-butyl group at N1 and a *p*-azidophenyl substituent at C3 as the synthetic objective (Scheme 1). We hypothesised that this structure would ensure enough thermal and chemical stability while also providing an anchor point for installation of different tags via the azide group. The synthetic route that we designed for obtaining **AM1** is depicted in Scheme 1.

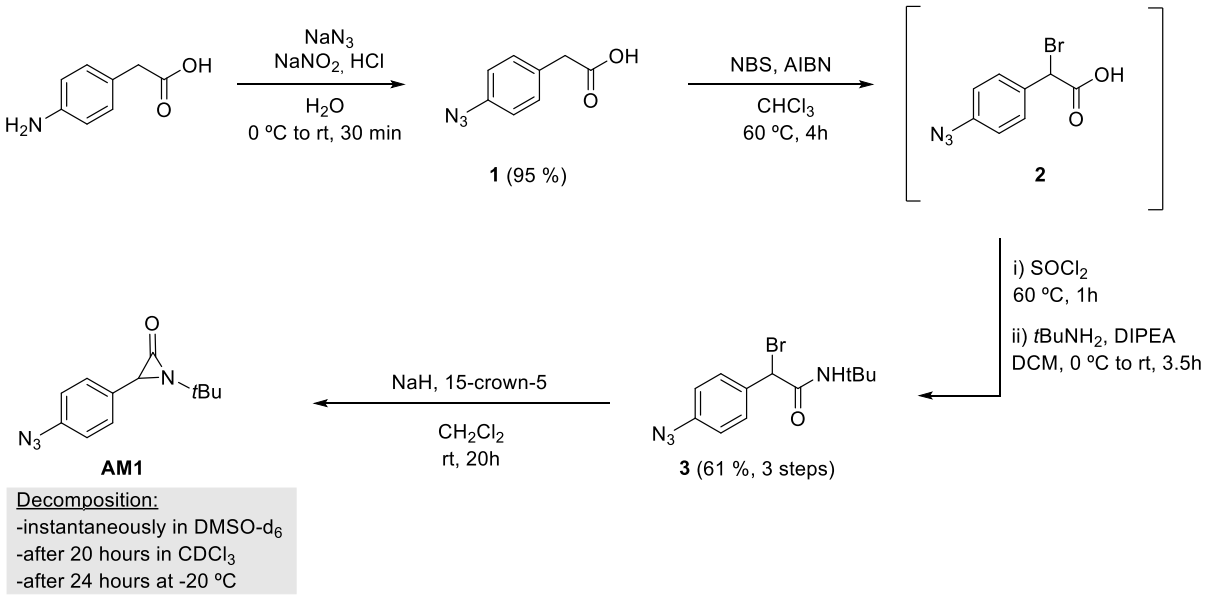

Scheme 1. Synthetic route to α-lactam **AM1**

Carboxylic acid **1** was obtained in 95 % yield from 4-aminophenylacetic acid by reaction with sodium azide through the corresponding diazonium salt.[40] Radical bromination of **1** yielded intermediate **2**[41] which was then transformed into the *N*-*t*-butyl amide **3** in a total yield of 61 % over three steps.[42,43] For cyclisation of the α-bromoamide **3**, we employed the protocol reported by V. Cesare *et al* using sodium hydride for deprotonation and 15-crown-5 as phase-transfer catalyst in dichloromethane.[44] However, even though formation of the α-lactam **AM1** could be detected in the crude reaction mixture by characteristic ^{1}H NMR and IR spectroscopic signatures, the compound proved extremely labile which ultimately prevented isolation of a pure sample. We observed that impure samples containing **AM1** in deuterated chloroform progressively decomposed so that after 20 hours the α-lactam could no longer be detected by ^{1}H-NMR spectroscopy. In comparison, the decomposition in deuterated dimethyl sulfoxide was instantaneous. Furthermore, no sign of **AM1** could be detected when a fresh ^{1}H-NMR sample in deuterated chloroform was prepared after 24 hours of storage of crude **AM1** at -20 °C. We attribute the high instability found for **AM1** to the stabilisation of an acyclic, planar or

quasi-planar, and charge-delocalised intermediate (or transition state) mediated by the presence of the aromatic substituent at C3[31,45] (Figure 2).

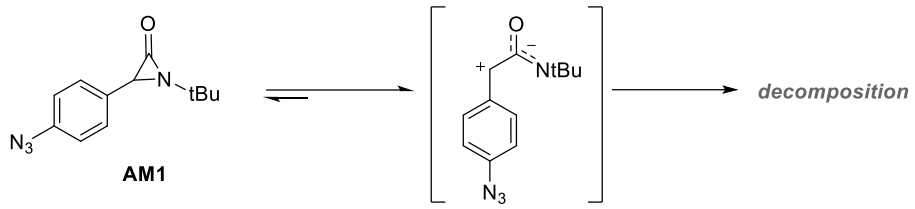

Figure 2. Charge delocalisation by the aromatic substituent in C3 contributes to the stabilisation of the acyclic form of **AM1**, making the α-lactam more reactive and more difficult to prepare.

These experiments clearly demonstrate that **AM1** (and closely related structures) are not relevant candidates for a biocompatible electrophile and underscore the challenge of navigating the delicate balance between reactivity and stability of α-lactams. The next candidate that we designed was **AM2** in which the presence of *tert*-butyl groups both at N1 and C3 were expected to sterically stabilise the structure and to also reduce the driving force for C3-cation formation (Figure 2). In addition, the PEG linker would serve to both increase aqueous solubility and provide an attachment point for an azide bioorthogonal tag. A convergent synthetic strategy that leads to **AM2** is shown in Scheme 2. As one component, α-bromoacyl chloride **4** was obtained in 94 % yield by bromination of 3,3-dimethylbutyryl chloride employing *N*-bromosuccinimide and catalytic amounts of hydrobromic acid.[46] Secondly, the azide-tagged tosylate **6** was synthesised from the corresponding alcohol **5** in 80 % yield and coupled to amino alcohol **7** under classical alkylation conditions with sodium hydride to afford amine **8** in 60 % yield. Compounds **5** and **7** were obtained by nucleophilic substitution of 2-(2-(2-chloroethoxy)ethoxy)ethan-1-ol and by $LiAlH_4$ reduction of 3-amino-3-methylbutyric acid, respectively.[47,48] Finally, the coupling reaction[43] between acyl chloride **4** and amine **8** led to the generation of the α-bromoamide **9** in 66 % yield, which would be subjected to cyclisation under basic conditions to afford the desired α-lactam **AM2**.

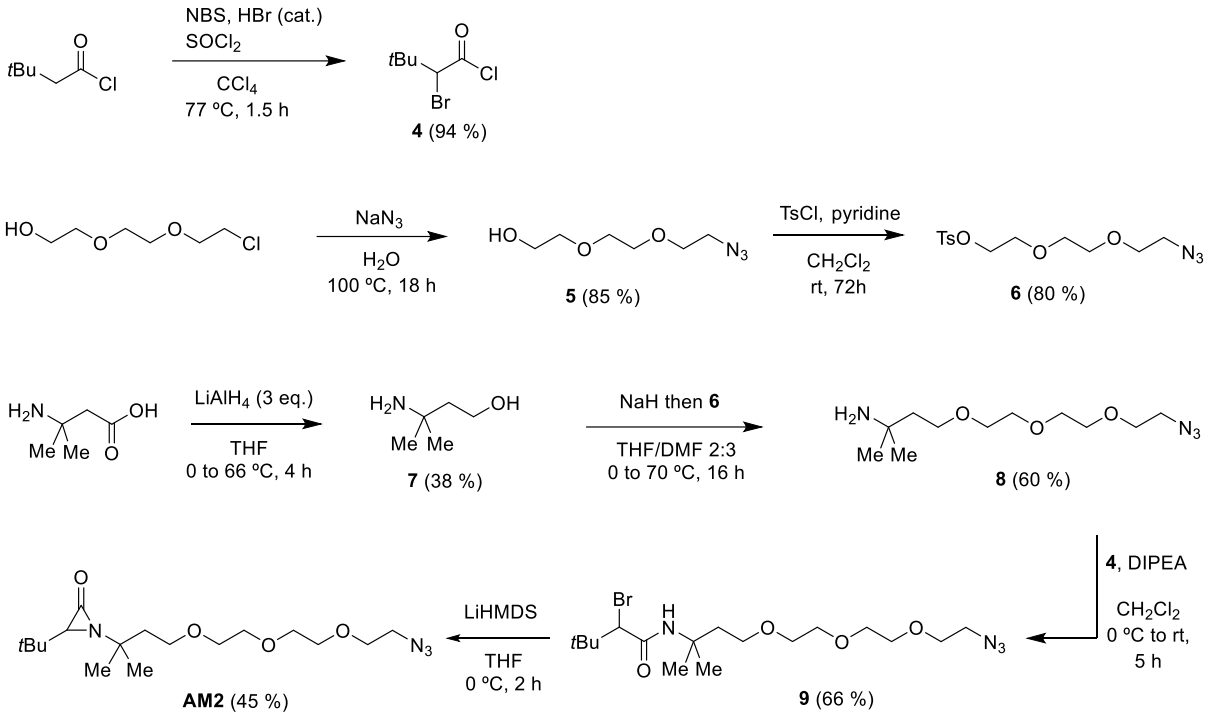

Scheme 2. Synthetic route to **AM2**.

The employment of sodium hydride as base in the presence of 15-crown-5 in dichloromethane at room temperature has been described as an easy and high-yielding procedure for the synthesis of α-lactams in the absence of undesired sideproducts.[44] However, when we attempted the former described conditions with **9**, the isolated yield for **AM2** was only 28 % while an unexpected compound was obtained as the major reaction product in 55 % yield (Table 1, entry 1). A thorough analysis of the ^{1}H-NMR, ^{13}C-NMR, IR and HRMS spectra allowed the unequivocal identification of this compound as isocyanide **12** (Figure 3). Isocyanides have previously been reported to result from thermal decomposition of α-lactams;[31,49] in the case of the analogous compound, 1,3-di-*tert*-butylaziridinone, *tert*-butyl isocyanide was obtained when the α-lactam was heated above 140 ºC.[35] Surprisingly, we obtained the isocyanide byproduct **12** under the cyclisation reaction conditions at room temperature. The formation of **12** may be rationalised through the generation of a putative iminooxirane intermediate **11** from the α-bromoamide anion **10** that results from the deprotonation of the α-bromoamide starting material **9** (Figure 3).[49–51] This intermediate can then further fragment into **12** and pivaldehyde although we did not attempt to verify the formation of the latter in these experiments.

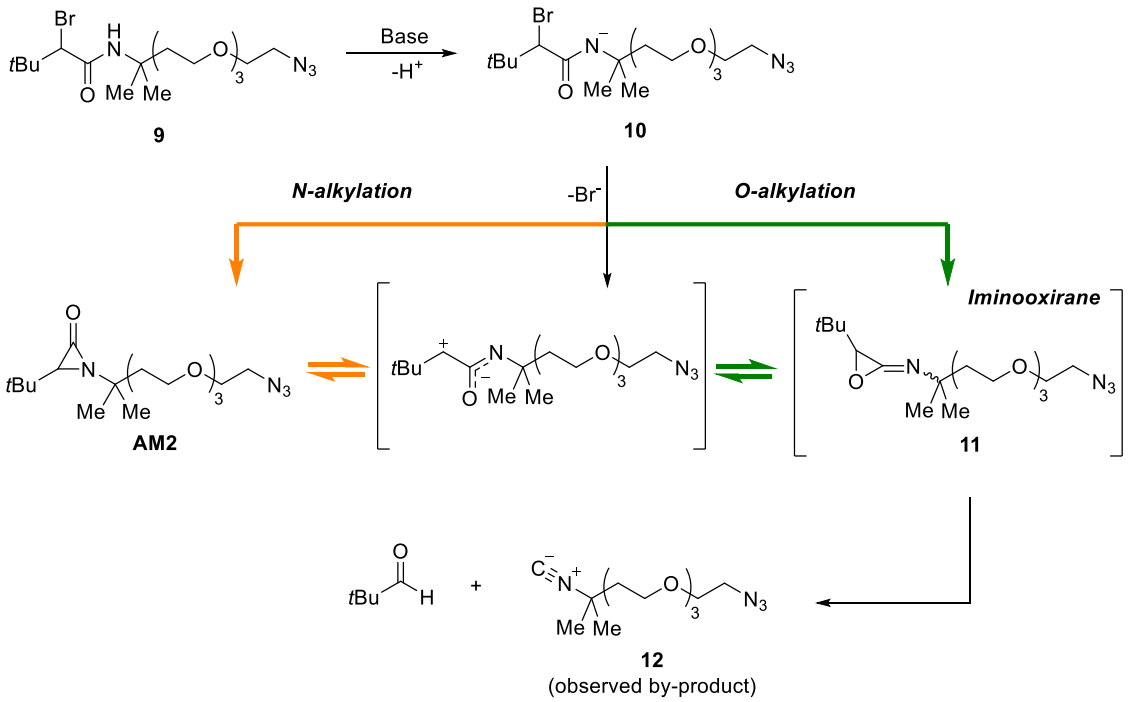

Figure 3. Proposed mechanism for the formation of isocyanide **12**.

As the generation of **12** during the synthesis of **AM2** hindered the isolation of the pure α-lactam, some modifications over the initially assayed conditions, as well as other different reaction conditions, were next assessed with the purpose of minimising the formation of this byproduct (Table 1). A decrease in stoichiometry of sodium hydride did not lead to any improvement in the reaction outcome (Table 1, entry 2). When the reaction temperature was lowered to 0 °C or 10 °C neither **AM2** nor **12** were obtained and the starting material remained unchanged (Table 1, entries 3 and 4). Alternatively, the employment of the classical general method for dehydrohalogenating α-haloamides with potassium *tert*-butoxide[31,35] provided **AM2** in low (11%) yield and isocyanide **12** in 55 % yield after 25 minutes of reaction (Table 1, entry 5). Finally, we attempted to decrease the reaction time to only 1 minute which afforded a ca. 1:1 mol mixture of α-lactam **AM2** and isocyanide **12** with a total yield of 51 % along with 15 % of unreacted starting material **9** (Table 1, entry 6). Thus, faced with this series of sub-optimal results, we decided to completely change the method by using lithium bis(trimethylsilyl)amide (LiHMDS), a non-nucleophilic strong base that, to our knowledge, had never previously been employed for the preparation of α-lactams. Initially, no progress in the reaction was detected at all with 1.5 equivalents of LiHMDS at -78 °C. In contrast, when 3.0 equivalents of base were added at 0 °C, the reaction was complete after 2 hours with 45 % isolated yield of **AM2** and less than 5 % yield of **12** as the outcome (Table 1, entry 8). This result represented both a crucial decrease in the amount of obtained by-product and provided the highest yield of **AM2** among all the assayed conditions.

Table 1. Reaction conditions for the cyclisation reaction of **9** to obtain **AM2**

Entry	Base	Conditions[a]	Yield (AM2)	Yield (12)
1	NaH (3 equiv.), 15-Crown-5 (0.25 equiv.)	CH_2Cl_2, rt, 22h	26 %[b] (28 %[c])	46 %[b] (55 %[c])
2	NaH (2 equiv.), 15-Crown-5 (0.25 equiv.)	CH_2Cl_2, rt, 20h	20 %[b]	58 %[b]
3	NaH (3 equiv.), 15-Crown-5 (0.25 equiv.)	CH_2Cl_2, 0 °C, 6h	ca. 0 %[d]	ca. 0 %[d]
4	NaH (3 equiv.), 15-Crown-5 (0.25 equiv.)	CH_2Cl_2, 10 °C, 16h	ca. 0 %[d]	ca. 0 %[d]
5	*t*BuOK (1.5 equiv.)	Et_2O, 0 °C, 25 min	11 %[e]	55 %[e]
6[e]	*t*BuOK (1.5 equiv.)	Et_2O, 0 °C, 1 min	25 %[b]	26 %[b]
7	LiHMDS (1.5 equiv.)	THF, -78 °C, 3h	ca. 0 %[d]	ca. 0 %[d]
8	LiHMDS (3 equiv.)	THF, 0 °C, 2h	45 %[c]	< 5 %[e]

[a] Reactions were carried out with 0.1 mmol of **9**. [b] Calculated by NMR (Internal Standard). [c] Isolated yield. [d] Estimated by TLC. [e] Estimated by NMR. [f] 15% of starting material remained in the crude reaction mixture.

Following the initial experiences with **AM1**, we were naturally sceptical about how **AM2** would behave. We found, however, that **AM2** could be purified by silica-gel column chromatography and was stable in deuterated chloroform for at least 7 days at room temperature. DMSO and acetonitrile solutions of **AM2** are stable in the freezer for at least 4 months. Additionally, the neat compound is completely stable for at least 2 months of storage at room temperature.

The synthesis of **AM2** thereby provides a readily available, thermally stable α-lactam that furthermore possess an azide tag. Next, we aimed to assess the aqueous stability of **AM2,** as well as its reactivity with nucleophiles, both of which would be critical indicators for potential use in different chemical biology applications.

Hydrolytic stability of AM2 and identification of decomposition pathways

Hydrolytic stability is an essential parameter in assessing the usefulness and relevancy of an electrophile as a molecular probe for chemical biology applications. With this aim, **AM2** was first incubated in aqueous buffer (pH 8, 55 °C) in preparative conditions. Under these conditions, the 2-hydroxyamide **13**, resulting from C3-N opening of the α-lactam, was the only detected compound in the crude reaction mixture along with the starting material **AM2**. The formation of **13** is in accordance with the generally observed reactivity trend between α-lactams and protic O-nucleophiles, mainly alcohols[31,36,37] (Scheme 3).

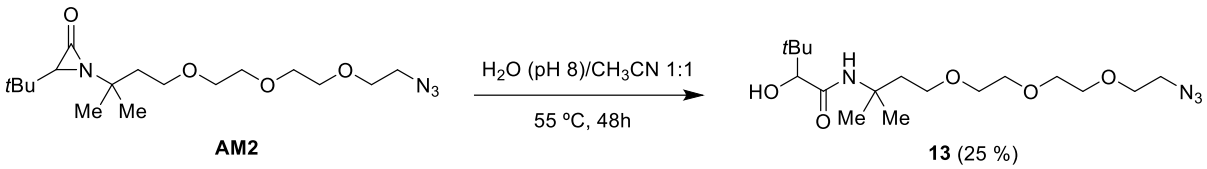

Scheme 3. Preparative synthesis of **13** from the α-lactam **AM2**

To obtain a clearer picture of the kinetics, we next conducted a systematic aqueous stability study of **AM2** in three different buffers: PBS (pH 7.4), potassium phosphate buffer (pH 8.1) and carbonate-bicarbonate buffer (pH 9.1). The depletion of **AM2** and the formation of the C3-N hydrolysis product **13** was monitored by HPLC (Figure 4). To our delight, **AM2** turned out to be stable for hours with obtained half-life times being 2.7 hours (pH 7.4), 12.7 hours (pH 8.1) and 56.0 hours (pH 9.1) thus showing a clear increase in the aqueous stability of the α-lactam in less acidic buffers (21-fold increase of half-life time from pH 7.4 to pH 9.1). At pH 9.1 the formation of **13,** as monitored by HPLC, correlates with 57 % of the end-point conversion of the α-lactam **AM2** (Figure 4, compare full and dashed purple curves), however, under less basic conditions, we were surprised to find that the main process responsible for the hydrolysis of **AM2** could not be the aqueous C3-N opening leading to compound **13** (only 4 % and 11 % end-point yield for **13** at pH 7.4 and 8.1, compared to conversions of 100 % and 70 % for **AM2**, respectively). Rather, one or more alternative decomposition mechanism(s) would have to be operating under these conditions.

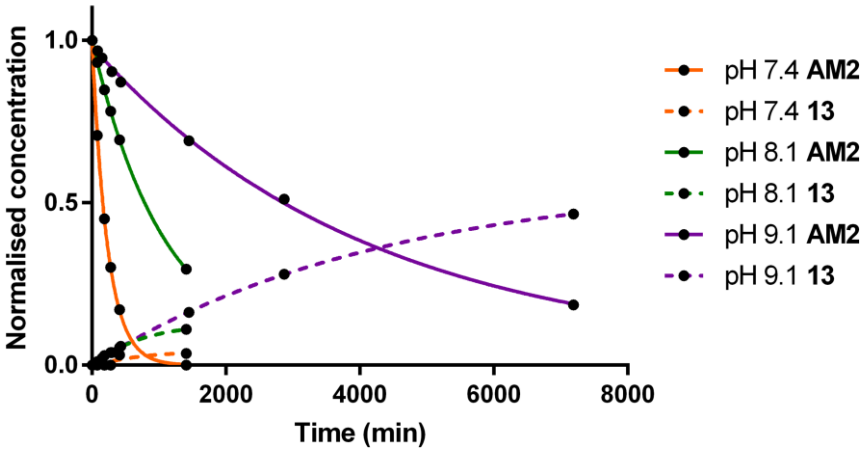

Figure 4. Stability of **AM2** in different aqueous buffers. HPLC-monitoring of the disappearance of **AM2** (solid lines) and the formation of **13** (dashed lines) measured in 100 µM samples of **AM2** in PBS (pH 7.4, orange), potassium phosphate buffer (pH 8.1, green) and carbonate-bicarbonate buffer (pH 9.1, purple). All samples contain 10 % acetonitrile. Data was fitted to an exponential curve (one phase decay).

There are two main decomposition pathways that have been previously observed in stable α-lactams without β-hydrogens at C3 upon subjection to different – relatively drastic – conditions.[52] On that basis, we can hypothesise the potential decomposition mechanisms of **AM2** under similar conditions (Figure 5). First, thermal decomposition of **AM2** would be expected to lead to isocyanide **12** and pivalaldehyde through the generation of an

intermediate iminooxirane **11** as discussed earlier.[31,49] The temperature at which this process takes place strongly depends on the stability of the α-lactam, but in the case of the analogous compound 1,3-di-*tert*-butylaziridinone it doesn´t start below 140 °C.[35] Alternatively, decarbonylation, which, to the best of our knowledge, has exclusively been reported for α-lactams upon reaction with strong acids in organic solvents, could induce formation of the immonium salt **14**[52] in the same manner that electron-induced fragmentation[45,53,54] and ultraviolet photolysis[55] would also do. In the presence of water, the immonium salt **14** would then hydrolyse to afford pivalaldehyde and the corresponding amine **8**. The formation of **12** or **8** is therefore diagnostic for each pathway. Trying to tease out these alternatives, we first found that amine **8** was detectable upon LC-MS analysis of the hydrolysis samples of **AM2** at both pH 7.4 and pH 8.1 while isocyanide **12** could not be detected (Figure S1). Furthermore, we cross-checked that aqueous samples of the hydrolysis product **13** and isocyanide **12** were both stable for at least 24 hours at pH 7.4 (Figure S2), thus discarding any kind of rapid decomposition mechanism that would involve these compounds and prevent their accumulation. To provide further support, we designed a trapping experiment to conclusively prove the presence of pivalaldehyde in aqueous samples of **AM2** at pH 7.4. Towards that end, we found that addition of phenylhydrazine after 24 hours of incubation resulted in the formation of the corresponding phenylhydrazone in at least 46 % yield relative to **AM2** as was confirmed by HPLC (Figure S3). All in all, these studies definitively demonstrate that the decarbonylative decomposition pathway, surprisingly, is the primary turnover-mediating pathway under neutral conditions which is extraordinarily mild compared to what has been previously reported for α-lactams in organic solvent.[52] Under more basic conditions, this decarbonylate pathway falls off and is replaced by a slower ring-opening reaction to form **13**.

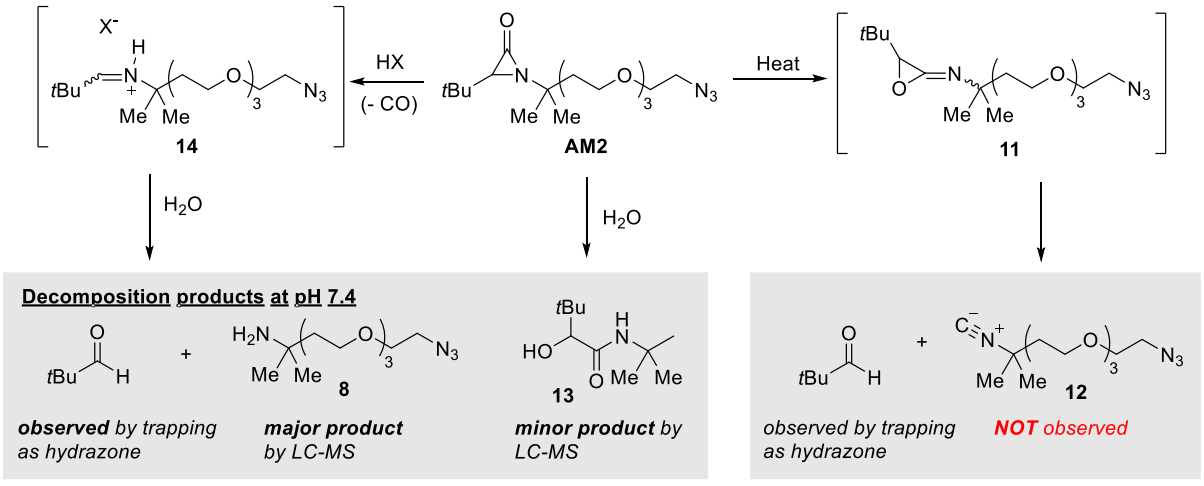

Figure 5. Potential decomposition pathways of **AM2**. In organic solvents, formation of isocyanides from stable α-lactams typically occurs at elevated temperatures whereas decarbonylation occurs in the presence of strong acids. In aqueous buffers at room temperature, **AM2** decomposes partly via decarbonylation to form amine **8** and direct hydrolysis (C3-N ring opening) to form **13**.

Reactivity of AM2 with thiols, alcohols, and amines

For chemical biology applications, an optimal balance between the hydrolytic stability of an electrophilic reagent and its reactivity must be achieved to ensure that amino acid modification occurs at an adequate rate. To evaluate the kinetics and potential outcome of the reaction between **AM2** and major proteinogenic nucleophiles, amines and thiols, we selected benzylamine and benzyl mercaptan as model nucleophiles and performed co-incubation studies under aqueous conditions in two different buffers: potassium phosphate buffer (pH 8.1) and carbonate-bicarbonate buffer (pH 9.1). The reaction kinetics were monitored by HPLC and the formed compounds were unequivocally confirmed by synthesis of references (Figure 6a,b). Similar to the reactivity observed in organic solvent, amide **15**, resulting from the C2-N opening of **AM2**, was the only reaction product detected during the incubation of the α-lactam with benzyl amine in aqueous media (Figure 6c). However, in the case of benzyl mercaptan, the outcome of the reaction drastically changed from organic to aqueous media. While the C3-N opening amide **16** was the only product resulting from the reaction between **AM2** and benzyl mercaptan in toluene at 90 ^{o}C (Figure 6b), the C2-N opening product, thioester **17,** was the only resulting product when the reaction was conducted in potassium phosphate buffer or carbonate-bicarbonate buffer (Figure 6c). We further found that **17** undergoes slow hydrolysis in water with a half-life time of 17 hours at pH 8.0 (Figure S4). Finally, we also evaluated the reactivity with a model alcohol nucleophile (benzyl alcohol) in carbonate-bicarbonate buffer (pH 9.1) but did not observe any change in the half-life time of **AM2** nor formation of new products, strongly indicating absence of reactivity between **AM2** and benzyl alcohol under the assayed conditions (Figure 6c).

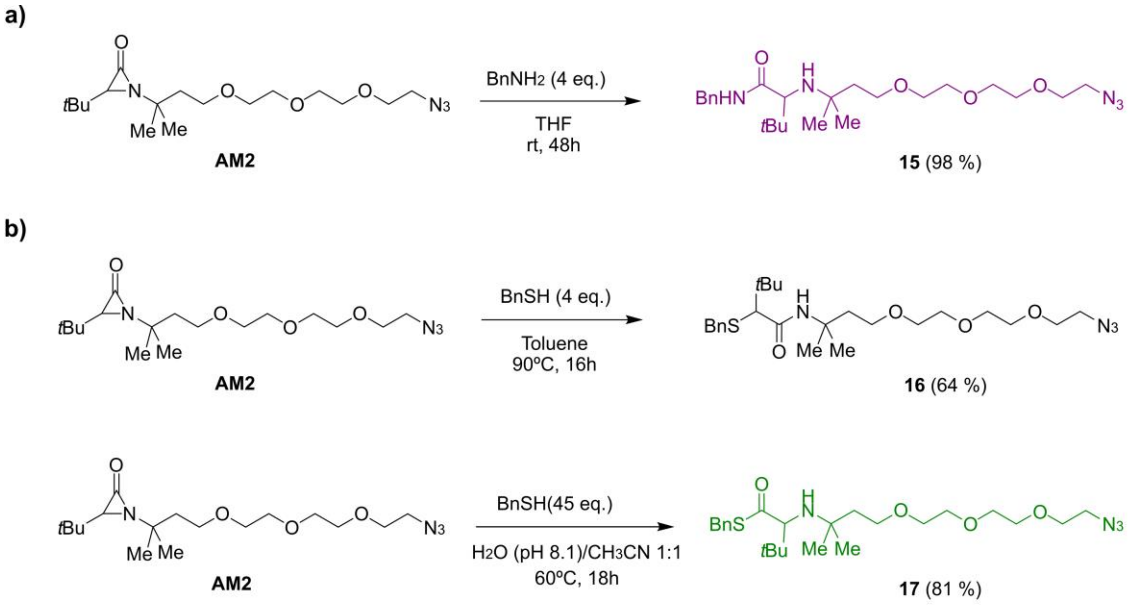

c)

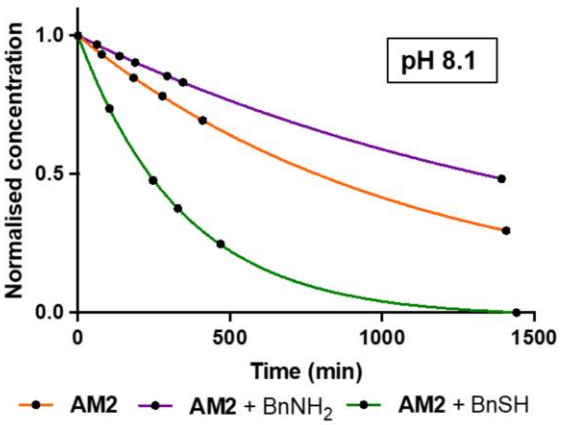

Sample	$T_{1/2}$ (AM2)	Yield (product, reaction time)
AM2	764 min	-
AM2 + $BnNH_2$	1380 min	17 % (**15**, 22.9 h)
AM2 + BnSH	231 min	34 % (**17**, 4.1 h)

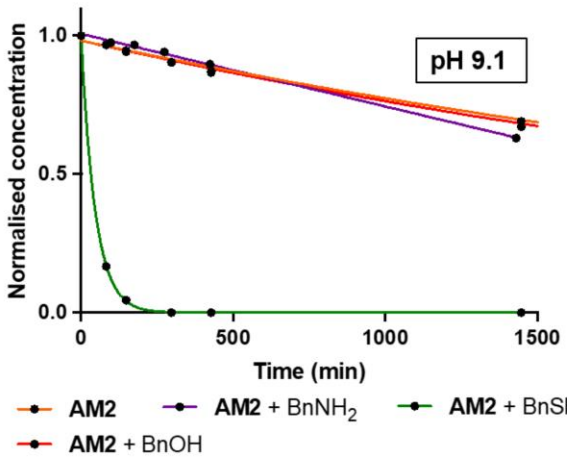

Sample	$T_{1/2}$ (AM2)	Yield (product, reaction time)
AM2	3357 min	-
AM2 + $BnNH_2$	2366 min	58 % (**15**, 71.7 h)
AM2 + BnSH	32 min	Quantitative (**17**, 2.5 h)
AM2 + BnOH	3349 min	0 % (24.1 h)

Figure 6. Reactivity study of **AM2** with nucleophiles. Preparative-scale reaction conditions between **AM2** and a) benzylamine or b) benzyl mercaptan used to identify and characterise the reaction products. c) HPLC-monitoring of the conversion of **AM2** (100 µM) incubated in potassium phosphate buffer (pH 8.1, left) and carbonate-bicarbonate buffer (pH 9.1, right) in the absence (orange) or in the presence of 4.5 mM benzylamine (purple), 4.5 mM benzyl mercaptan (green) or 4.5 mM of benzyl alcohol (red). Samples contain 10 % acetonitrile. Data was fitted to an exponential curve (one phase decay). Half-life times ($T_{1/2}$) of **AM2** and product yields at selected times are also indicated for all tested conditions.

Taken together, the observed reaction kinetics (half-life time of **AM2**) and product yields in aqueous buffers are clear indicators of higher reactivity of the α-lactam **AM2** with benzyl mercaptan relative to benzylamine. (Figure 6c). This effect is especially noticeable at pH 9.1 in carbonate-bicarbonate buffer, where the reaction with benzyl mercaptan occurred with a half-life time of only 32 minutes, which is 74 times faster compared to the reaction between **AM2** and benzylamine at the same conditions (Figure 6c, right). In potassium phosphate buffer (Figure 6c, left) benzylamine is even contributing to increase the stability of the α-lactam as a consequence of a slight increment of 0.5 units in the pH of the sample.

Peptide-functionalisation with AM2

As the next rational step in the assessment of the applicability of **AM2** for covalent modification of proteins, we examined the reactivity with peptides under aqueous conditions. In this regard, we selected octreotide and oxytocin as model cyclic peptides as they both contain a disulfide bridge along with additional nucleophilic side chains. Conditional reduction of the disulfide bridge, e.g. with TCEP, can then trigger the presence of free thiols which we speculated would primarily mediate reactivity with **AM2**. In practice, we incubated both peptides with **AM2** under reducing and non-reducing conditions in borate buffer (pH 9.0) and analysed the outcome of the different reactions by LC-MS. In the absence of TCEP, no new products could be identified and only the starting peptides were observed by LC-MS (data not shown). In contrast, in the presence of TCEP both peptides were observed to react with **AM2** affording both mono- and diconjugates consisting of one molecule of reduced peptide attached to one or two molecules of **AM2**, respectively (Figure 7a). The conjugated peptides were detected in the UV-chromatogram as close duplicated peaks that we speculate represent the different diastereomers of the same conjugate (Figures 7b and 7c). Subsequent MS fragmentation analysis of the conjugates clearly indicated that the α-lactam units are connected to both peptides through cysteine residues (See Supporting Information for additional details). Additionally, the MS fragmentation data strongly suggests that **AM2** is attached to oxytocin and octreotide as a thioester (See Supporting Information for additional details), which is in line with the mode of reactivity observed between **AM2** and benzyl mercaptan under aqueous conditions (see Figure 6). Interestingly, we did not observe any indications of thioester to amide rearrangements to migrate the conjugate to the N-terminus of oxytocin.[56]

All in all, these experiments demonstrate that the α-lactam, **AM2,** is a biologically relevant electrophile with surprising aqueous stability.

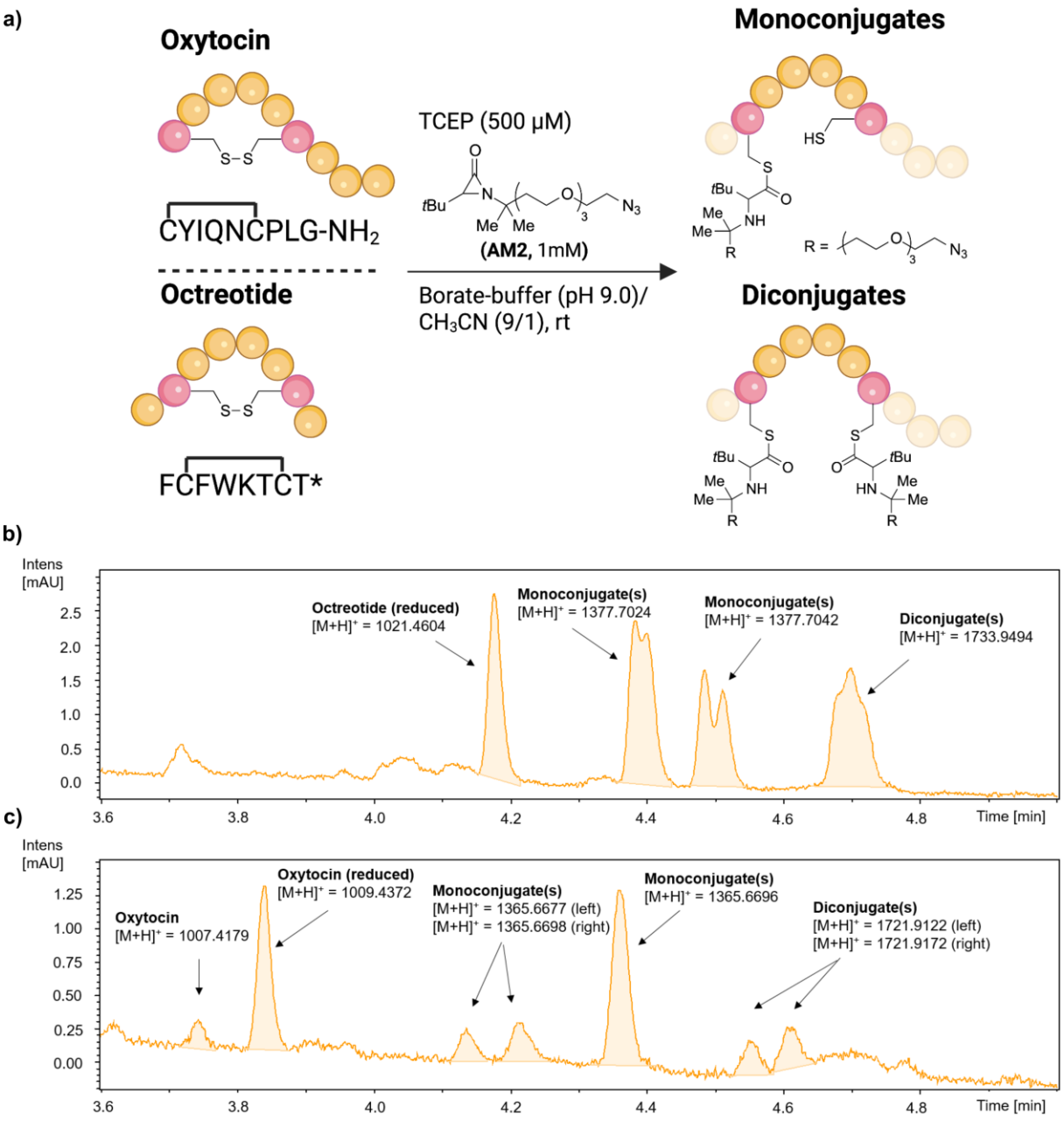

Figure 7. LC-MS study of the reactivity of **AM2** with peptides. a) Mode of reactivity of **AM2** with cyclic peptides octreotide and oxytocin: mono- and diconjugate species are formed under reducing conditions (in the presence of TCEP). Figure created with BioRender.com. UV-chromatogram (280 nm) measured after 3 hours of incubation of 100 µM b) octreotide or c) oxytocin with 500 µM TCEP and 1 mM **AM2** in borate buffer (pH 9.0)/CH_3CN 9:1 at room temperature. Samples were diluted (1:10) in Milli-Q water/CH_3CN 9:1 before the LC-MS analysis. T* = threoninol at the C-terminus.

Proteome profiling with AM2 reveals conjugation to and inhibition of human carboxylesterase 1

Having obtained evidence that **AM2** indeed possesses the properties expected for a biologically relevant electrophile, we next sought to assess its reactivity in more complex biological samples: the proteome from mammalian cells. Initially, we incubated live HCT116 colon-cancer cells, HeLa cell lysate, and U2OS bone-cancer cell lysate with increasing concentrations of **AM2**, followed by a workflow involving conjugation of a FAM-alkyne fluorophore to the protein-bound **AM2** via copper-catalysed azide-alkyne cycloaddition (CuAAC). Finally, protein separation by SDS-PAGE and imaging of FAM-fluorescence allowed for qualitative visualisation of stable covalent targets of **AM2**. However, no clear bands could be observed for **AM2** concentrations below 100 µM on any of the resulting gels (Figures S5-S6) contrary to the significant thiol-reactivity observed in buffer. One explanation could be that any potential thioester-conjugates of **AM2** are too labile to survive sample processing. However, when we conducted the same experiment in HepG2 liver-cancer cells, a single, intense band (at ca. 60 kDa) was observed at concentrations below 1 µM in both cell lysate (Figure 8a) and live cells (Figure S7). Interestingly, the 60 kDa-band appeared to saturate in the relatively low nM range, and the kinetics of binding were exceptionally fast as substantial labelling was observed within just a few minutes of incubation with 1 µM of **AM2** (Figure 8b) in a subsequent experiment.

To identify the 60 kDa protein, we conducted a pull-down experiment by **AM2**-treatment of live HepG2 cells, CuAAC-conjugation to biotin-alkyne, and enrichment using streptavidin beads (Figure S8). The eluted proteins were separated by SDS-PAGE and stained, which allowed for visual observation of the 60 kDa band. Excision of the band, followed by in-gel digestion and LC-MS/MS analysis identified the specific protein as human liver carboxylesterase 1 (CES1, P23141), an enzyme belonging to the serine hydrolase superfamily. During the last two decades, the significant pharmacological relevance of CES1 has been well established, as it is one of the main enzymes responsible for the activation of ester-containing prodrugs, as well as detoxification of xenobiotics and the hydrolysis of endogenous lipids.[57] Due to the pharmacological and physiological significance, the development of chemical tools to modulate and study CES1 activity remains of interest to this day.[58,59] Interestingly, CES1 does not contain any free cysteine residues which would be the expected primary target sites of **AM2**, and we therefore decided to focus on this unexpected interaction in subsequent experiments. First, we validated CES1 as the **AM2**-target protein by western blotting using a CES1-specific antibody (Figure 8d). Next, by mining the LC-MS/MS data we found that the specific **AM2**-target site is on the peptide covering positions 199-237 in the protein sequence. The active site serine (Ser221), which together with His467 and Glu354 form the catalytic triad of CES1, is thus part of this modified sequence. However, no direct MS evidence of modification of Ser221 was obtained (See Figures S21-23 for additional details).

To gain insight into the binding site, and to further probe the modulatory effects of **AM2** on CES1 function, we turned to fluorophosphonate probes which, as already mentioned, are state-of-the-art reagents for activity-based profiling of serine hydrolases.[9,10] Towards this end, we synthesised fluorophosphonate-containing probes **FP1** and **FP2** (Figure 8e, and Supporting

Information),[60] with **FP1** incorporating an azide tag for bioorthogonal manipulations, and **FP2** as an equivalent untagged derivative.

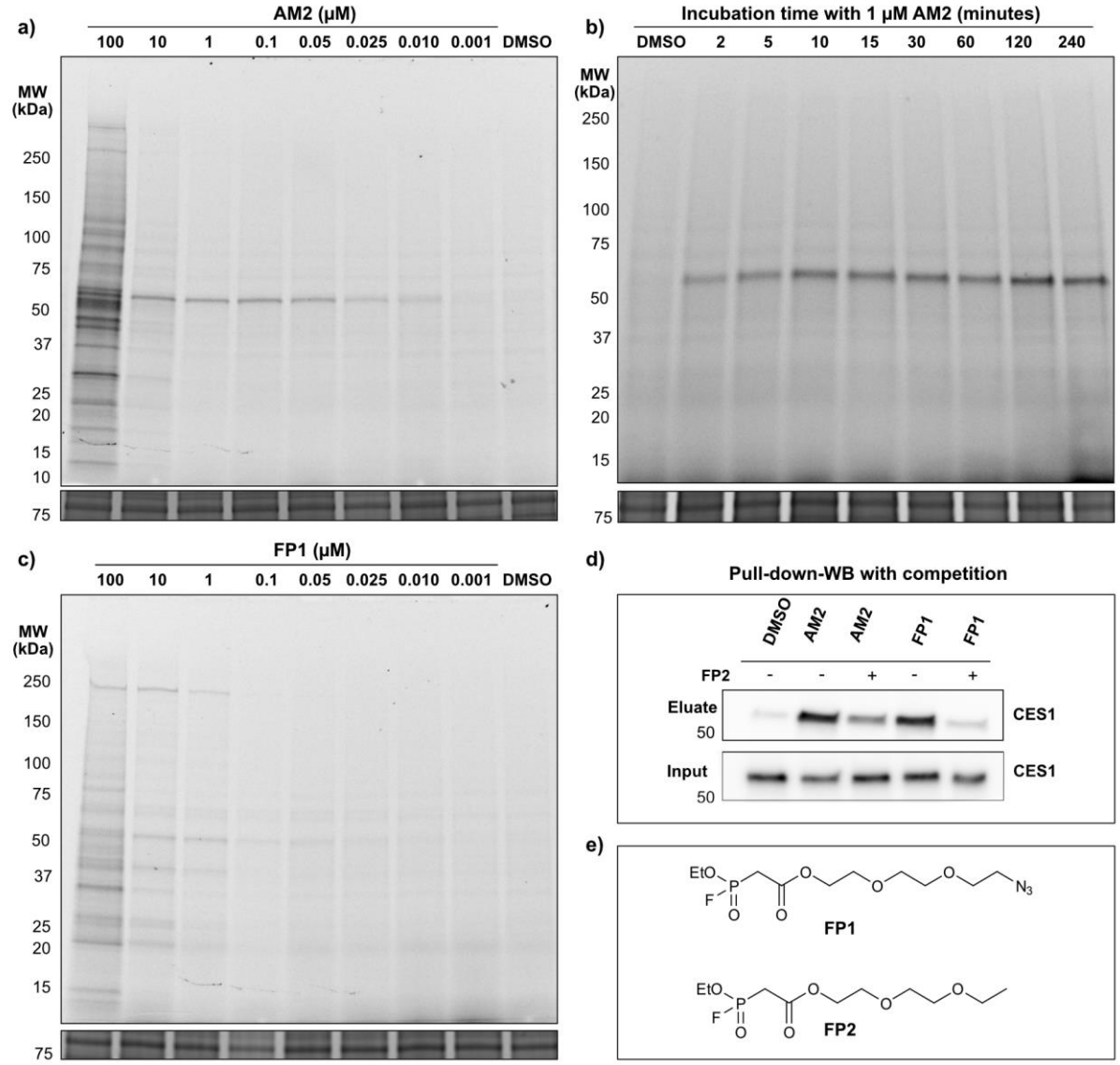

Figure 8. Proteomic profiling and biological experiments with **AM2**. a) Representative FAM-fluorescence gel from **AM2** labelling in HepG2 lysate with 2 h of incubation. b) FAM-fluorescence gel after incubation with 1 μM **AM2** in HepG2 lysate for varying amounts of time. c) Representative FAM-fluorescence gel from **FP1** labelling in HepG2 cells as in a. d) Representative results from competition experiments where samples were incubated 100 μM **FP2** for 30 minutes prior to 2 h of incubation with 1 μM **AM2** or **FP1**, followed by pull-down and western-blotting. e) Structures of fluorophosphonate probes **FP1** and **FP2**.

We employed **FP1** in a pull-down-CES1 western blotting experiment from HepG2 cell lysate which demonstrated that this probe, similarly to **AM2**, strongly enriched CES1 (Figure 8d). As expected, pre-treatment with an excess of unlabelled fluorophosphonate **FP2** was found to reduce **FP1**-mediated CES1 binding, but, interestingly, **FP2**-pre-treatment also efficiently

competed **AM2**-mediated CES1 binding (Figure 8d). This strongly suggests that **AM2** does in fact target the active site serine (Ser221) of CES1.

We then surveyed the global binding targets of **FP1** in HepG2 lysate using an in gel-fluorescence readout (Figure 8c). While the labelling pattern obtained for **FP1** did indeed contain a band in the mass-range expected for CES1 (ca. 60 kDa), several additional bands were observed at concentrations where only the CES1 band is evident for **AM2** (Figure 8a,c). Likewise, additional bands could be observed for **FP1** upon incubation with both HeLa and U2OS cell lysate (Figure S9), even at concentrations below 100 µM, where no such binding was evident for **AM2**. As **FP1** is known to target serine hydrolases broadly, promiscuous binding is expected and, when compared to **AM2**, it is clear that the latter targets CES1 with both high selectivity and potency, as well as a lack of overt toxicity (Figure S10).

Next, we reasoned that if **AM2** does form a stable, covalent bond in the CES1 active site, then it should be possible to demonstrate inhibition of CES1 activity. To test this hypothesis, we immunofixated CES1 from HepG2 cells in antibody-coated wells of a 96-well plate prior to the addition of a mixture containing 4-nitrophenyl butyrate (4-NPB) and varying concentrations of **AM2** (Figure 9a). As the CES1-mediated hydrolysis of 4-NPB results in the formation of 4-nitrophenol, CES1 activity was measured as the increase in absorbance at 402 nm (due to the formation of 4-nitrophenolate). In accordance with the hypothesis of active-site binding, **AM2** displayed effectively complete inhibition of CES1 activity at 10 µM - which was also the case for **FP1** (Figure S11) - as well as notable, time-dependent inhibition down to 100 nM (Figure 9b).

As the shape of the progress curves and the observed time-dependent decrease in IC_{50} value (Figures 9b, 9c, and S11) indicated two-step covalent irreversible inhibition (at least within the timeframe of the experiment), we utilised the IC_{50}-shift method developed by Krippendorf *et al.*,[61] as presented by Mons *et al.*,[62] to determine a k_{inact}/K_I parameter for the **AM2**-CES1 inhibition. To this end, the initial 31 minutes of data, where no substrate depletion can be observed (the uninhibited control is strictly linear) was used (Figure S11). This analysis yielded a k_{inact} value of of $1.7 \cdot 10^{-2}$ s^{-1} (SEM: $2.6 \cdot 10^{-3}$ s^{-1}) and a K_I value of $2.0 \cdot 10^{-6}$ M (SEM: $2.6 \cdot 10^{-7}$ M), resulting in a second order inactivation constant, k_{inact}/K_I, of $8.8 \cdot 10^{3}$ M^{-1} s^{-1} (SEM: $1.8 \cdot 10^{3}$ M^{-1} s^{-1}), which is comparable to the values reported for the covalent carbamate CES1 inhibitors JZL184 and URB597 by Crow *et al*.[63]

Finally, we expected the CES1-**AM2** covalent species to be a hindered ester and as such capable of undergoing hydrolysis – even if this process occurred at such a relatively slow pace that **AM2** effectively behaved as an irreversible inhibitor in our previous experiments. Indeed, we were able to observe partial (roughly 45 %) reactivation of CES1 upon washout of **AM2** followed by two hours of incubation (37 °C with shaking at 300 rpm) in buffer (Figure S11). This is in accordance with the hypothesis of ester formation and suggests that **AM2** is a 'slow-substrate' covalent inhibitor.[64]

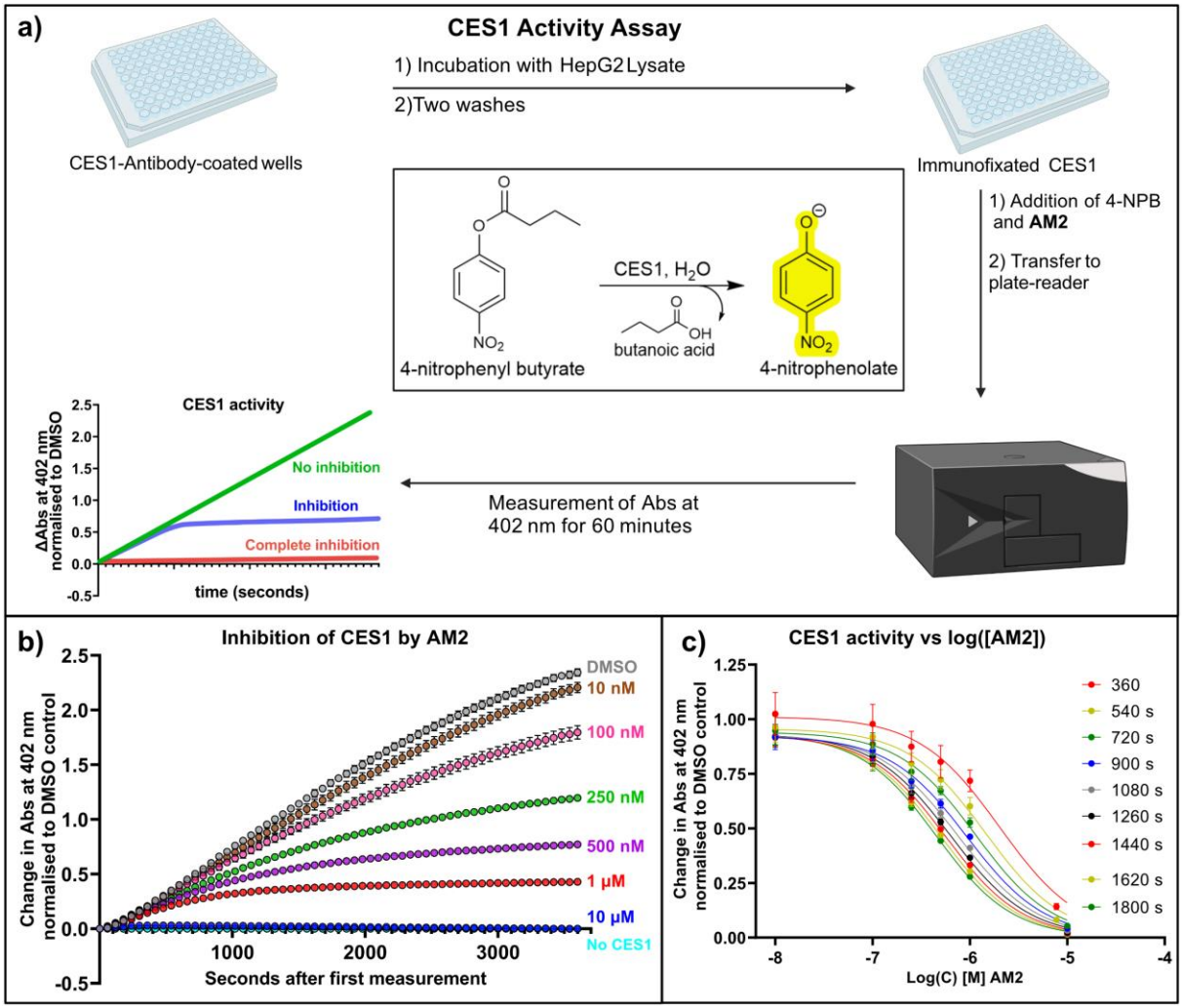

Figure 9. Inhibition of CES1 by **AM2**. a) Simplified Illustration of the CES1-activity assay utilised to investigate inhibition by **AM2**. Figure created with BioRender.com b) Results from the inhibition assay using 5 mM 4-NPB and varying concentrations of **AM2**. Each point represents the mean of three technical replicates. Absorbance was measured at 402 nm c) CES1 activity vs log10-transformed AM2 concentration at different time points. CES1 activity was measured as change in absorbance at 402 nm from the first measurement until the time points indicated, normalised to the change observed for the DMSO controls. Each point represents the mean of three technical replicates. IC_{50} values were determined through nonlinear regression (variable slope – four parameters) in GraphPad Prism 9.4.0.

Due to the multifaceted role of CES1 in the metabolism of both xeno- and endobiotic species, inhibition of this particular enzyme is a matter of both complexity and pharmacological relevance. On one hand, CES1 has been demonstrated to facilitate the inactivation of several therapeutics, including the antiplatelet agent clopidogrel for which coadministration of a CES1 inhibitor (bis(4-nitrophenyl) phosphate) significantly decreased inactivation,[65] indicating the possible use of CES1 inhibitors as co-drugs to improve pharmacokinetics of certain CES1-inactivated therapeutics.[66] However, the prevalence of CES1-activated prodrugs already on the market should be cause for caution, as utilising CES1 inhibitors as drugs or co-drugs could lead to drug-drug interactions with unintended, and potentially harmful changes in

pharmacokinetics arising as a result.[67] Interestingly, daily oral administration of a novel Ces3 (the murine ortholog of CES1) inhibitor was previously found to ameliorate obesity-diabetes in obese-diabetic db/db mice.[68] As the same study also found the levels of human CES1 activity to be increased in obese individuals and patients with type 2 diabetes, selective CES1 inhibitors may hold potential as drug candidates in their own right. It is therefore of interest to understand the different factors that underlie the apparent high selectivity of **AM2** for CES1 over other serine hydrolases (Figure 8a,c).[69] Regardless of their potential as drugs or co-drugs, CES1 inhibitors serve additional purposes, namely as molecular tools in the further elucidation of the role of CES1 in endobiotic lipid metabolism and in determining the contribution of CES1 to the overall metabolism of drug candidates in human tissue preparations, thus aiding the deconvolution of complex processes.[70] **AM2** may contribute to such studies in the future.

CONCLUSION

In conclusion, we have reported the first example of an α-lactam electrophilic reagent, **AM2**, that is compatible with aqueous buffers and can be employed for protein and peptide functionalisation. Our studies have e.g. revealed an α-lactam decomposition pathway, via decarbonylation, that operates under mild aqueous conditions and have furthermore demonstrated that α-lactams, *in vitro* and in cells, can react with both thiol, amine, and alcohol nucleophiles. With respect to the latter, we surprisingly found that **AM2** targets and inhibits the serine hydrolase enzyme CES1 in HepG2 cells with high selectivity and efficiency. Our future studies will be directed at further expansion of the structural space around electrophilic α-lactams and their different applications in covalent chemical biology.

ASSOCIATED CONTENT

Supporting Information: general methods, synthetic procedures, LC-MS/MS and pull-down analysis, figures and spectra (PDF).

ACKNOWLEDGEMENTS

This project has received funding from the European Research Council (ERC) under the European Union's Horizon 2020 research and innovation programme (grant agreement number 865738). Financial support from the Novo Nordisk Foundation (grant NNF19OC0054782) is acknowledged.

TABLE OF CONTENTS GRAPHIC

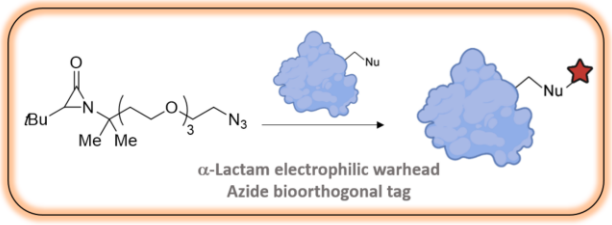

- Compatible with aqueous buffers
- Peptide functionalisation
- *In vitro* reactivity with thiols and amines
- Selective targeting and inhibition of CES1

REFERENCES

(1) Singh, J.; Petter, R. C.; Baillie, T. A.; Whitty, A. The Resurgence of Covalent Drugs. *Nat. Rev. Drug Discov.* **2011**, *10*, 307–317.

(2) Vita, E. De. 10 Years into the Resurgence of Covalent Drugs. *Future Med. Chem.* **2021**, *13*, 193–210.

(3) Zhang, T.; Hatcher, J. M.; Teng, M.; Gray, N. S.; Kostic, M. Recent Advances in Selective and Irreversible Covalent Ligand Development and Validation. *Cell Chem. Biol.* **2019**, *26*, 1486–1500.

(4) Backus, K. M.; Correia, B. E.; Lum, K. M.; Forli, S.; Horning, B. D.; González-Páez, G. E.; Chatterjee, S.; Lanning, B. R.; Teijaro, J. R.; Olson, A. J.; Wolan, D. W.; Cravatt, B. F. Proteome-Wide Covalent Ligand Discovery in Native Biological Systems. *Nature* **2016**, *534*, 570–574.

(5) Roberts, A. M.; Miyamoto, D. K.; Huffman, T. R.; Bateman, L. A.; Ives, A. N.; Akopian, D.; Heslin, M. J.; Contreras, C. M.; Rape, M.; Skibola, C. F.; Nomura, D. K. Chemoproteomic Screening of Covalent Ligands Reveals UBA5 as a Novel Pancreatic Cancer Target. *ACS Chem. Biol.* **2017**, *12*, 899–904.

(6) Resnick, E.; Bradley, A.; Gan, J.; Douangamath, A.; Krojer, T.; Sethi, R.; Geurink, P. P.; Aimon, A.; Amitai, G.; Bellini, D.; Bennett, J.; Fairhead, M.; Fedorov, O.; Gabizon, R.; Gan, J.; Guo, J.; Plotnikov, A.; Reznik, N.; Ruda, G. F.; Díaz-Sáez, L.; Straub, V. M.; Szommer, T.; Velupillai, S.; Zaidman, D.; Zhang, Y.; Coker, A. R.; Dowson, C. G.; Barr, H. M.; Wang, C.; Huber, K. V. M.; Brennan, P. E.; Ovaa, H.; Von Delft, F.; London, N. Rapid Covalent-Probe Discovery by Electrophile-Fragment Screening. *J. Am. Chem. Soc.* **2019**, *141*, 8951–8968.

(7) Keeley, A.; Petri, L.; Ábrányi-Balogh, P.; Keserű, G. M. Covalent Fragment Libraries in Drug Discovery. *Drug Discov. Today* **2020**, *25*, 983–996.

(8) Cordon, M. B.; Jacobsen, K. M.; Nielsen, C. S.; Hjerrild, P.; Poulsen, T. B. Forward Chemical Genetic Screen for Oxygen-Dependent Cytotoxins Uncovers New Covalent Fragments That Target GPX4. *ChemBioChem* **2022**, *23*, e202100253.

(9) Liu, Y.; Patricelli, M. P.; Cravatt, B. F. Activity-Based Protein Profiling: The Serine Hydrolases. *Proc. Natl. Acad. Sci. U. S. A.* **1999**, *96*, 14694–14699.

(10) Cravatt, B. F.; Wright, A. T.; Kozarich, J. W. Activity-Based Protein Profiling: From Enzyme Chemistry to Proteomic Chemistry. *Annu. Rev. Biochem.* **2008**, *77*, 383–414.

(11) Weerapana, E.; Wang, C.; Simon, G. M.; Richter, F.; Khare, S.; Dillon, M. B. D.; Bachovchin, D. A.; Mowen, K.; Baker, D.; Cravatt, B. F. Quantitative Reactivity Profiling Predicts Functional Cysteines in Proteomes. *Nature* **2010**, *468*, 790–795.

(12) Zanon, P. R. A.; Yu, F.; Musacchio, P. Z.; Lewald, L.; Zollo, M.; Krauskopf, K.; Mrdović, D.; Raunft, P.; Maher, T. E.; Cigler, M.; Chang, C. J.; Lang, K.; Toste, F. D.; Nesvizhskii, A. I.; Hacker, S. M. Profiling the Proteome-Wide Selectivity of Diverse Electrophiles. *ChemRxiv. Cambridge: Cambridge Open Engage* **2021**, Non peer-reviewed preprint.

(13) Zanon, P. R. A.; Lewald, L.; Hacker, S. M. Isotopically Labeled Desthiobiotin Azide

(IsoDTB) Tags Enable Global Profiling of the Bacterial Cysteinome. *Angew. Chem. Int. Ed.* **2020**, *59*, 2829–2836.

(14) Hansen, B. K.; Loveridge, C. J.; Thyssen, S.; Wørmer, G. J.; Nielsen, A. D.; Palmfeldt, J.; Johannsen, M.; Poulsen, T. B. STEFs: Activated Vinylogous Protein-Reactive Electrophiles. *Angew. Chem. Int. Ed.* **2019**, *58*, 3533–3537.

(15) Wørmer, G. J.; Hansen, B. K.; Palmfeldt, J.; Poulsen, T. B. A Cyclopropene Electrophile That Targets Glutathione S-Transferase Omega-1 in Cells. *Angew. Chem. Int. Ed.* **2019**, *58*, 11918–11922.

(16) Gehringer, M.; Laufer, S. A. Emerging and Re-Emerging Warheads for Targeted Covalent Inhibitors: Applications in Medicinal Chemistry and Chemical Biology. *J. Med. Chem.* **2019**, *62*, 5673–5724.

(17) Bach, K.; Beerkens, B. L. H.; Zanon, P. R. A.; Hacker, S. M. Light-Activatable, 2,5-Disubstituted Tetrazoles for the Proteome-Wide Profiling of Aspartates and Glutamates in Living Bacteria. *ACS Cent. Sci.* **2020**, *6*, 546–554.

(18) Ahangarpour, M.; Kavianinia, I.; Hume, P. A.; Harris, P. W. R.; Brimble, M. A. N-Vinyl Acrylamides: Versatile Heterobifunctional Electrophiles for Thiol–Thiol Bioconjugations. *J. Am. Chem. Soc.* **2022**, *144*, 13652–13662.

(19) Istrate, A.; Geeson, M. B.; Navo, C. D.; Sousa, B. B.; Marques, M. C.; Taylor, R. J.; Journeaux, T.; Oehler, S. R.; Mortensen, M. R.; Deery, M. J.; Bond, A. D.; Corzana, F.; Jiménez-Osés, G.; Bernardes, G. J. L. Platform for Orthogonal N-Cysteine-Specific Protein Modification Enabled by Cyclopropenone Reagents. *J. Am. Chem. Soc.* **2022**, *144*, 10396–10406.

(20) Reddi, R. N.; Resnick, E.; Rogel, A.; Rao, B. V.; Gabizon, R.; Goldenberg, K.; Gurwicz, N.; Zaidman, D.; Plotnikov, A.; Barr, H.; Shulman, Z.; London, N. Tunable Methacrylamides for Covalent Ligand Directed Release Chemistry. *J. Am. Chem. Soc.* **2021**, *143*, 4979–4992.

(21) Silva, M. J. S. A.; Faustino, H.; Coelho, J. A. S.; Pinto, M. V.; Fernandes, A.; Compañón, I.; Corzana, F.; Gasser, G.; Gois, P. M. P. Efficient Amino-Sulfhydryl Stapling on Peptides and Proteins Using Bifunctional NHS-Activated Acrylamides. *Angew. Chem. Int. Ed.* **2021**, *60*, 10850–10857.

(22) Stieger, C. E.; Park, Y.; de Geus, M. A. R.; Kim, D.; Huhn, C.; Slenczka, J. S.; Ochtrop, P.; Müchler, J. M.; Süssmuth, R.; Broichhagen, J.; Baik, M.-H.; Hackenberger, C. DFT-Guided Discovery of Ethynyl-Triazolyl-Phosphinates as Modular Electrophiles for Chemoselective Cysteine Bioconjugation and Profiling. *Angew. Chem. Int. Ed.* **2022**, e202205348.

(23) Tang, K. C.; Maddox, S. M.; Backus, K. M.; Raj, M. Tunable Heteroaromatic Azoline Thioethers (HATs) for Cysteine Profiling. *Chem. Sci.* **2022**, *13*, 763–774.

(24) Rempel, B. P.; Withers, S. G. Covalent Inhibitors of Glycosidases and Their Applications in Biochemistry and Biology. *Glycobiology* **2008**, *18*, 570–586.

(25) McGregor, L. M.; Jenkins, M. L.; Kerwin, C.; Burke, J. E.; Shokat, K. M. Expanding the Scope of Electrophiles Capable of Targeting K-Ras Oncogenes. *Biochemistry* **2017**, *56*,

3178–3183.

(26) Lin, S.; Yang, X.; Jia, S.; Weeks, A. M.; Hornsby, M.; Lee, P. S.; Nichiporuk, R. V.; Iavarone, A. T.; Wells, J. A.; Toste, F. D.; Chang, C. J. Redox-Based Reagents for Chemoselective Methionine Bioconjugation. *Science* **2017**, *355*, 597–602.

(27) Christian, A. H.; Jia, S.; Cao, W.; Zhang, P.; Meza, A. T.; Sigman, M. S.; Chang, C. J.; Toste, F. D. A Physical Organic Approach to Tuning Reagents for Selective and Stable Methionine Bioconjugation. *J. Am. Chem. Soc.* **2019**, *141*, 12657–12662.

(28) Ma, N.; Hu, J.; Zhang, Z. M.; Liu, W.; Huang, M.; Fan, Y.; Yin, X.; Wang, J.; Ding, K.; Ye, W.; Li, Z. 2H-Azirine-Based Reagents for Chemoselective Bioconjugation at Carboxyl Residues Inside Live Cells. *J. Am. Chem. Soc.* **2020**, *142*, 6051–6059.

(29) Smith, E.; Collins, I. Photoaffinity Labeling in Target-and Binding-Site Identification. *Future Med. Chem.* **2015**, *7*, 159–183.

(30) West, A. V.; Muncipinto, G.; Wu, H. Y.; Huang, A. C.; Labenski, M. T.; Jones, L. H.; Woo, C. M. Labeling Preferences of Diazirines with Protein Biomolecules. *J. Am. Chem. Soc.* **2021**, *143*, 6691–6700.

(31) Lengyel, I.; Sheehan, J. C. A-Lactams (Aziridinones). *Angew. Chemie Int. Ed. English* **1968**, *7*, 25–36.

(32) Hubschwerlen, C. β-Lactam Antibiotics. In *Comprehensive Medicinal Chemistry II*; Elsevier Ltd, 2007; pp 479–518.

(33) Baumgarten, H. E. Reactions of Amines. X. 1-t-Butyl-3-Phenylaziridinone. *J. Am. Chem. Soc.* **1962**, *84*, 4975–4976.

(34) Benitez, M.; Wang, Y. D.; Lengyel, I.; Fitzsimmons, M.; Cesare, V. About the First Stable α-Lactam with a Secondary Alkyl Substituent in Position Three: 3-Isopropyl-1-Triphenylmethylaziridinone. *J. Heterocycl. Chem.* **2018**, *55*, 2877–2882.

(35) Sheehan, J. C.; Beeson, J. H. α-Lactams. IV. A Stable α-Lactam, 1,3-Di-t-Butylaziridinone. *J. Am. Chem. Soc.* **1967**, *89*, 362–366.

(36) Talaty, E. R.; Yusoff, M. M. Regioselectivity in Nucleophilic Ring-Opening of Aziridinones. *Chem. Commun.* **1998**, No. 9, 985–986.

(37) Hoffman, R. V.; Zhao, Z.; Costales, A.; Clarke, D. Origins of Regioselectivity in the Reactions of α-Lactams with Nucleophiles. Two Distinct Acid-Catalyzed Pathways Involving O- and N-Protonation. *J. Org. Chem.* **2002**, *67*, 5284–5294.

(38) Tantillo, D. J.; Houk, K. N.; Hoffman, R. V.; Tao, J. Origins of Regio- and Stereoselectivity in Acid-Promoted Reactions of α-Lactams. *J. Org. Chem.* **1999**, *64*, 3830–3837.

(39) Lengyel, I.; Cesare, V.; Chen, S.; Taldone, T. About the Factors Which Govern the Ring-Opening of α-Lactams with Benzylamine: I. The Relative Stability of the α-Lactam and the Substituent on Nitrogen. *Heterocycles* **2002**, *57*, 677–695.

(40) Chamni, S.; He, Q. L.; Dang, Y.; Bhat, S.; Liu, J. O.; Romo, D. Diazo Reagents with Small Steric Footprints for Simultaneous Arming/SAR Studies of Alcohol-Containing Natural Products via O-H Insertion. *ACS Chem. Biol.* **2011**, *6*, 1175–1181.

(41) MacKiewicz, N.; Bark, T.; Cao, B.; Delaire, J. A.; Riehl, D.; Ling, W. L.; Foillard, S.; Doris, E. Fullerene-Functionalized Carbon Nanotubes as Improved Optical Limiting Devices. *Carbon* **2011**, *49*, 3998–4003.

(42) Chiba, S.; Zhang, L.; Lee, J. Y. Copper-Catalyzed Synthesis of Azaspirocyclohexadienones from α-Azido- N -Arylamides under an Oxygen Atmosphere. *J. Am. Chem. Soc.* **2010**, *132*, 7266–7267.

(43) Box, H. K.; Upul Kumarasinghe, K. G.; Nareddy, R. R.; Akurathi, G.; Chakraborty, A.; Raji, B.; Rowland, G. B. Rhodium-Catalyzed Coupling of α-Lactams with Indole Derivatives. *Tetrahedron* **2014**, *70*, 9709–9717.

(44) Cesare, V.; Lyons, T. M.; Lengyel, I. A High-Yielding General Synthesis of α-Lactams. *Synthesis (Stuttg).* **2002**, No. 12, 1716–1720.

(45) Talaty, E. R.; Utermoehlen, C. M. Isolation and Stability of an α-Lactam with a New Substitution Pattern: 3-Phenyl-1,3-Di-t-Butylaziridin-2-One. *J. Chem. Soc. D* **1970**, No. 8, 473–474.

(46) Lengyel, I.; Cesare, V.; Taldone, T.; Uliss, D. The Synthesis, Physical, and Spectral Properties, and Some Reactions of a New Stable Bis-α-Lactam (Aziridinone) with a Terpene Skeleton. *Synth. Commun.* **2001**, *31*, 3671–3683.

(47) Xiao, Q.; Bécar, N. A.; Brown, N. P.; Smith, M. S.; Stern, K. L.; Draper, S. R. E.; Thompson, K. P.; Price, J. L. Stapling of Two PEGylated Side Chains Increases the Conformational Stability of the WW Domain via an Entropic Effect. *Org. Biomol. Chem.* **2018**, *16*, 8933–8939.

(48) Torre, O.; Gotor-Fernández, V.; Gotor, V. Lipase-Catalyzed Resolution of Chiral 1,3-Amino Alcohols: Application in the Asymmetric Synthesis of (S)-Dapoxetine. *Tetrahedron Asymmetry* **2006**, *17*, 860–866.

(49) Sheehan, J. C.; Lengyel, I. A. The Formation of an Isocyanide and a Ketone from an α-Haloamide. *J. Am. Chem. Soc.* **1964**, *86*, 746–747.

(50) Maran, F. Electrochemical and Stereochemical Investigation on the Mechanism of the Decay of 2-Halo Amide Anions. The Intermediacy of Aziridinones. *J. Am. Chem. Soc.* **1993**, *115*, 6557–6563.

(51) Cohen, A. D.; Showalter, B. M.; Toscano, J. P. Time-Resolved IR Detection and Study of an Iminooxirane Intermediate. *Org. Lett.* **2004**, *6*, 401–403.

(52) Lengyel, I.; Cesare, V.; Taldone, T. A Direct Link between the Passerini Reaction and α-Lactams. *Tetrahedron* **2004**, *60*, 1107–1124.

(53) Lengyel, I.; Uliss, D. B. The Synthesis and Spectral Properties of a New Stable α-Lactam: 1-(1-Adamantyl)-3-t-Butylaziridinone. *Chem. Commun.* **1968**, No. 24, 1621–1622.

(54) Lengyel, I.; Uliss, D. B.; Mark, R. V. Charge Migration in Odd- and Even-Electron Fragment Ions. The Mass Spectrum of a Bisaziridinone. *J. Org. Chem.* **1970**, *35*, 4077–4084.

(55) Sheehan, J. C.; Nafissi-V, M. M. α-Lactams. VI. Photochemistry of α-Lactams. *J. Am. Chem. Soc.* **1969**, *91*, 1176–1178.

(56) Conibear, A. C.; Watson, E. E.; Payne, R. J.; Becker, C. F. W. Native Chemical Ligation in Protein Synthesis and Semi-Synthesis. *Chem. Soc. Rev.* **2018**, *47*, 9046–9068.

(57) Wang, D.; Zou, L.; Jin, Q.; Hou, J.; Ge, G.; Yang, L. Human Carboxylesterases: A Comprehensive Review. *Acta Pharm. Sin. B* **2018**, *8*, 699–712.

(58) Singh, A.; Gao, M.; Beck, M. W. Human Carboxylesterases and Fluorescent Probes to Image Their Activity in Live Cells. *RSC Med. Chem.* **2021**, *12*, 1142–1153.

(59) Wang, D. D.; Zou, L. W.; Jin, Q.; Hou, J.; Ge, G. B.; Yang, L. Recent Progress in the Discovery of Natural Inhibitors against Human Carboxylesterases. *Fitoterapia* **2017**, *117*, 84–95.

(60) Wang, C.; Abegg, D.; Dwyer, B. G.; Adibekian, A. Discovery and Evaluation of New Activity-Based Probes for Serine Hydrolases. *ChemBioChem* **2019**, *20*, 2212–2216.

(61) Krippendorff, B. F.; Neuhaus, R.; Lienau, P.; Reichel, A.; Huisinga, W. Mechanism-Based Inhibition: Deriving Ki and Kinact Directly from Time-Dependent IC50 Values. *J. Biomol. Screen.* **2009**, *14*, 913–923.

(62) Mons, E.; Roet, S.; Kim, R. Q.; Mulder, M. P. C. A Comprehensive Guide for Assessing Covalent Inhibition in Enzymatic Assays Illustrated with Kinetic Simulations. *Curr. Protoc.* **2022**, *2*, e419.

(63) Crow, J. A.; Bittles, V.; Borazjani, A.; Potter, P. M.; Ross, M. K. Covalent Inhibition of Recombinant Human Carboxylesterase 1 and 2 and Monoacylglycerol Lipase by the Carbamates JZL184 and URB597. *Biochem. Pharmacol.* **2012**, *84*, 1215–1222.

(64) Tuley, A.; Fast, W. The Taxonomy of Covalent Inhibitors. *Biochemistry* **2018**, *57*, 3326–3337.

(65) Zhu, H. J.; Wang, X.; Gawronski, B. E.; Brinda, B. J.; Angiolillo, D. J.; Markowitz, J. S. Carboxylesterase 1 as a Determinant of Clopidogrel Metabolism and Activations. *J. Pharmacol. Exp. Ther.* **2013**, *344*, 665–672.

(66) Makhaeva, G. F.; Lushchekina, S. V.; Boltneva, N. P.; Serebryakova, O. G.; Kovaleva, N. V.; Rudakova, E. V.; Elkina, N. A.; Shchegolkov, E. V.; Burgart, Y. V.; Stupina, T. S.; Terentiev, A. A.; Radchenko, E. V.; Palyulin, V. A.; Saloutin, V. I.; Bachurin, S. O.; Richardson, R. J. Novel Potent Bifunctional Carboxylesterase Inhibitors Based on a Polyfluoroalkyl-2-Imino-1,3-Dione Scaffold. *Eur. J. Med. Chem.* **2021**, *218*, 113385.

(67) Song, Y. Q.; Jin, Q.; Wang, D. D.; Hou, J.; Zou, L. W.; Ge, G. B. Carboxylesterase Inhibitors from Clinically Available Medicines and Their Impact on Drug Metabolism. *Chem. Biol. Interact.* **2021**, *345*, 109566.

(68) Dominguez, E.; Galmozzi, A.; Chang, J. W.; Hsu, K. L.; Pawlak, J.; Li, W.; Godio, C.; Thomas, J.; Partida, D.; Niessen, S.; O'Brien, P. E.; Russell, A. P.; Watt, M. J.; Nomura, D. K.; Cravatt, B. F.; Saez, E. Integrated Phenotypic and Activity-Based Profiling Links Ces3 to Obesity and Diabetes. *Nat. Chem. Biol.* **2014**, *10*, 113–121.

(69) Faucher, F.; Bennett, J. M.; Bogyo, M.; Lovell, S. Strategies for Tuning the Selectivity of Chemical Probes That Target Serine Hydrolases. *Cell Chem. Biol.* **2020**, *27*, 937–952.

(70) Shimizu, M.; Fukami, T.; Nakajima, M.; Yokoi, T. Screening of Specific Inhibitors for

Human Carboxylesterases or Arylacetamide Deacetylase. *Drug Metab. Dispos.* **2014**, *42*, 1103–1109.